

TECHNICAL NOTE

Measurements of flow structure in the stagnation zone of impinging free-surface liquid jets

J. STEVENS† and B. W. WEBB

Department of Mechanical Engineering, Brigham Young University, Provo, UT 84602, U.S.A.

(Received 10 February 1993 and in final form 27 May 1993)

INTRODUCTION

IMPINGING jets are used in a variety of heat and mass transfer applications including the glass and metal industries for cooling, in the paper and textile industries for drying, and thermal control of high heat flux electronics. Inasmuch as the heat and mass transfer beneath an impinging jet depend on the nature of the flow field, a full understanding of the flow is a prerequisite to understanding the associated transport phenomena of other scalar quantities. The objective of this research was to rigorously characterize the stagnation region flow field of a normally impinging free-surface liquid jet formed from a fully-developed pipe flow.

Several analytical studies have addressed the problem of jet impingement. The related case of an infinite, laminar stagnation flow, which has an exact solution for the Navier–Stokes equations, has been treated [1, 2]. A similarity solution was determined where the shape of the velocity profiles depended only on the coordinate normal to the plane. This solution reveals the boundary layer to be of constant thickness.

There is only limited work on the flow structure of free-surface liquid jets. Olsson and Turkdogan examined experimentally the radial flow field of an impinging liquid jet [3]. Nozzle-to-plate spacings of 26 and 64 diameters were used, and experiments included a variety of liquids with varying viscosities. Azuma and Hoshino reported LDV measurements inside the radial liquid layer formed by placing axisymmetric nozzles close to a flat plate [4]. Nozzle-to-plate spacings of 0.07, 0.08 and 0.3 diameters were investigated. However, no measurements were made of the stagnation zone. Measured free-surface velocity distributions have been reported in ref. [5]. Experimental characterization of the turbulent flow structure in the radial layer (outside the stagnation zone) of free-surface jets was presented in ref. [6]. More recently, the turbulent flow structure was characterized experimentally for the stagnation zone of free-surface liquid jets issuing from a variety of nozzle types by Stevens *et al.* [7]. These measurements accompanied local heat transfer measurements made in the stagnation zone [8].

It is clear from the preceding discussion that little has been done in the experimental characterization of the flow field of free-surface liquid jets. The objective of this study was to experimentally explore the stagnation zone flow structure of impinging free-surface liquid jets issuing from fully-developed nozzles by measuring local instantaneous liquid velocities throughout the stagnation region as a function of nozzle size and flow rate.

EXPERIMENTAL APPARATUS AND METHOD

Liquid velocities were measured with a TSI laser-Doppler velocimeter with the optics configured for backscatter operation. A tenth-wave, front surface mirror was used to reflect the laser beams through a glass plate onto which the free-surface liquid jet was impinging, such that the diagnostic volume was positioned inside the jet. The measurement volume was moved relative to the stationary experimental setup by moving the entire LDV system on a three-axis traversing table with 0.1 mm resolution in each direction. Only the radial component of velocity was measured in this study. Further details of the experimental apparatus are available elsewhere [7, 9].

For each flow and nozzle configuration, a square matrix of local velocity and turbulence measurements was taken in a plane perpendicular to the impingement surface and intersecting the stagnation streamline of the jet. For each horizontal (radial) traverse, the measurement volume was initially positioned slightly to one side of the stagnation streamline, then moved radially across that streamline out to $r/d \approx 0.5$ (r and d being the radial coordinate and the nozzle diameter, respectively). The radial extent of the velocity measurements was limited at vertical locations well away from the impingement surface due to the intersection of the laser beams with the liquid jet boundary. The stagnation streamline was determined for each radial scan by interpolating between discrete measurement locations to locate the point where the measured radial velocity vanished. The vertical location of the measurement position relative to the impingement surface was determined by lowering the LDV probe volume until the Doppler signal matched the shift frequency used, indicating zero velocity. This study revealed that three thousand data points were adequate in characterizing the flow statistics. For most of the data reported here a single nozzle-to-plate spacing of $z_0/d = 1$ was used. Here, z_0 is the dimensional nozzle-to-plate spacing. This was adopted to avoid problems with jet destabilization at higher nozzle-to-plate spacings. However, the effect of increased z_0/d on the flow structure was also investigated for a single Reynolds number ($Re = V_j d/\nu$, V_j being the jet exit velocity) for $z_0/d = 2$ and 4.

In order to determine the flow regime under consideration, an approximation was made for the boundary layer thickness under the finite liquid jet using the relationship between the hydrodynamic and thermal boundary layer thicknesses, δ and δ_T , respectively, $\delta/\delta_T \sim Pr^{0.42}$, where Pr is the fluid Prandtl number [2]. The thermal boundary layer thickness may be approximated as $\delta_T = k(T_S - T_\infty)/q''$, where k is the fluid thermal conductivity, T_S and T_∞ are the local heated surface and impinging jet temperatures, respectively, and q'' is the imposed plate heat flux. An empirical correlation for the Nusselt number from Stevens and Webb [10] then results in estimated maximum hydrodynamic boundary layer thick-

† Currently at Department of Mechanical Engineering, Mississippi State University, Mississippi State, MS 39762, U.S.A.

nesses for each nozzle between 0.04 and 0.24 mm. Since the effective length of the measurement volume was approximately 0.3 mm on the major axis, no more than a single measurement in the vertical direction could possibly come from within the viscous boundary layer. Although this estimate may be very crude, even if it were in error by an order of magnitude, less than 6% of the data would still originate from inside the boundary layer. Thus, the velocity measurements reported here are almost exclusively taken from outside the hydrodynamic boundary layer. Therefore, these measurements pertain to the inviscid, free-surface liquid jet flow regime, and do not directly illustrate the boundary layer flow under the jet.

Maximum uncertainty in the average jet velocity (measured with the flowmeters) is estimated to be 7%. Uncertainty in the local velocity measurements (measured with the LDV) is estimated to be less than 5%. The uncertainty in location of each measurement is estimated to be ± 0.3 mm in the axial direction normal to the plate (z) and ± 0.1 mm in the radial direction (r).

RESULTS AND DISCUSSION

A sample of the velocity measurements for two nozzle sizes and different flow rates is shown in Fig. 1, where the normalized radial velocity, u/V_j , is plotted as a function of the dimensionless radial coordinate, r/d . The measured mean velocity exhibits a near-linear variation with radial coordinate, with the exception of a slight downward concavity observed for $z/d > 0.3$. At larger z/d , the mean radial velocities vanish as expected; the flow is essentially a purely axial flow at vertical locations far from the impingement plate. These data are representative of experimental measurements at all Reynolds numbers and nozzle diameters studied. No boundary layer effects are expected nor observed in Fig. 1, since, as was discussed previously, all measurements presented here were taken from locations outside the hydrodynamic boundary layer.

Since the radial velocities vary nearly linearly with the radial coordinate, and vanish at the jet centerline, each radial scan can be characterized by the slope of the profile. This suggests that the near-plate flow field may be represented by an equation of the form

$$u = f(z)r \quad (1)$$

where $f(z)$ is an unknown function of the axial coordinate, z . Some insight into the form of the unknown function, $f(z)$ may be gained by considering the continuity equation, and

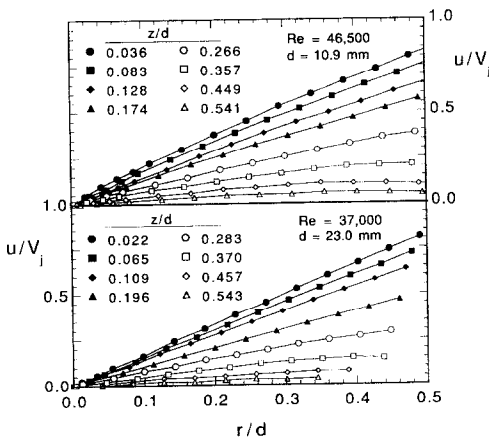


FIG. 1. Sample distributions of the measured mean radial velocity for two nozzle diameters and two Reynolds numbers.

the two momentum equations in their inviscid form. When combined with equation (1) and appropriate boundary conditions, these equations require that $f'' = 0$, so that the governing equations for inviscid flow may be satisfied by a polynomial, $f(z)$ of order one or zero [9]. Thus

$$u = (mz + b)r \quad (2)$$

where m and b are constants to be determined. In dimensionless terms

$$\frac{u}{V_j} = \left[\left(\frac{md^2}{V_j} \right) \left(\frac{z}{d} \right) + \left(\frac{bd}{V_j} \right) \right] r \quad (3)$$

This conclusion is supported by the experimental results shown in Fig. 2. The dimensionless velocity gradient, $d(u/V_j)/d(r/d)$, is plotted as a function of z/d and nozzle size for a wide range of Reynolds number. This parameter has relevance to the stagnation point heat transfer coefficient, as suggested by previous analytical and experimental work on free-surface liquid jet impingement heat transfer [7, 8, 11]. The gradient appears to fall in a single relatively tight band without any consistent effect of either nozzle size or Reynolds number. The data follow a straight line for $0 < z/d < 0.5$. The scatter in the $d = 2.1$ mm data are believed to be due to higher uncertainty in the calculation of the dimensionless gradient and determination of the vertical location. Near $z/d = 0.5$, the band of gradient data bends sharply and approaches zero for larger z/d . This deviation from linear behavior in the mean velocity gradient near $z/d = 0.5$ can be explained by noting that in Fig. 1 the profiles exhibit increasing curvature for $z/d > 0.3$. Any curvature renders the preceding analysis inapplicable. Other nozzle types have also been observed to exhibit a linear radial relationship [7]. A least-squares fit of the data in Fig. 2 for $0 \leq z/d \leq 0.5$ results in $md^2/V_j = -3.66$ and $bd/V_j = 1.83$. Interestingly, the value of the velocity gradient at the wall observed in these data, $bd/V_j = 1.83$, agrees exactly with that from an analytical study of flow under laminar free-surface liquid jets [11].

Most of the measurements in this study were made at a nozzle-to-plate spacing of $z_0/d = 1$. Figure 2 also shows data collected for $z_0/d = 2$ and 4 for a jet with diameter $d = 14$ mm in the Reynolds number range $25800 \leq Re \leq 46400$. Clearly, the influence of nozzle-to-plate spacing on measured velocity gradients is minimal for the range of z_0/d and Re studied. Significantly larger Reynolds numbers and/or nozzle-to-plate spacings would be expected to result in differences from the reported data due to gravitational effects and/or jet instabilities.

Two additional observations may be made regarding Figs. 1 and 2. First, the measured flow field for an impinging free-

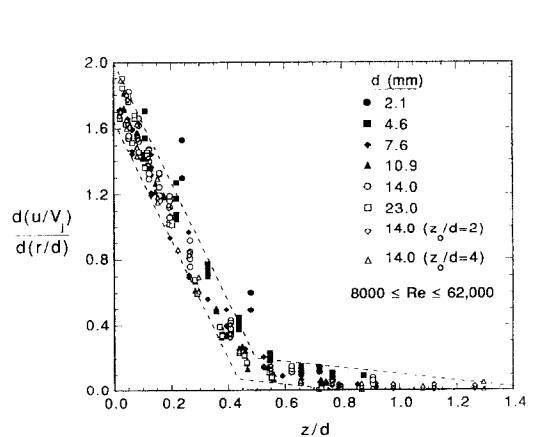


FIG. 2. Dependence of the mean radial velocity gradient on z/d for all nozzle diameters and Reynolds numbers investigated.

surface liquid jet, which can be successfully modeled near the plate by equation (2), is not described by the infinite stagnation flow stream function, $\Psi = cr^2z$, where c is constant [2]. This is significant since many heat and mass transport analyses use the infinite stagnation flow field as an approximation to the finite jet flow field near the stagnation point. A different stream function, $\Psi = r^2(mz^2/2 + bz)$, can be generated from equation (2) which is suggested by the finite jet data.

Second, the information presented in Fig. 2 permits estimation of the vertical distance from the impingement plate where the deceleration of the approaching jet is initiated. Let this distance be denoted $z_\infty (< z_0)$, and consider the limiting case of a radially uniform axial velocity (v) profile and negligible acceleration due to gravity. At the point where the jet begins to decelerate, $z = z_\infty$, the following conditions hold:

$$v_{z=z_\infty} = -V_j \quad \text{and} \quad \left. \frac{dv}{dz} \right|_{z=z_\infty} = 0. \quad (4)$$

These conditions may be applied to the flow field described by equation (2), and with the experimentally determined parameters $md^2/V_j = -3.66$ and $bd/V_j = 1.83$ (from Fig. 2), an estimate of the deceleration distance $z_\infty/d \approx 0.5$ is determined. The impingement plate thus influences the approaching jet only in a vertical region extending approximately half the jet diameter from the plate. This value of z_∞/d also holds for nozzle-to-plate spacings in the range $1 \leq z_0/d \leq 4$, as demonstrated in Fig. 2. It should be emphasized that this analysis applies only to jets for which the gravitational acceleration and jet contraction are negligible.

For the majority of the measurements of this study Reynolds numbers were chosen so that the acceleration in the jet due to gravity would be negligible (less than 1% of the average jet exit velocity). However, a set of measurements was conducted at deliberately low Reynolds numbers to study the effect of gravity-induced jet contraction. Figure 3 illustrates the variation of the normalized radial velocity component with radial position for $Re = 2600$ and 5200 , $d = 14$ mm, $z_0/d = 1$. The velocity distributions are qualitatively similar to such plots at higher Re , with the exception that the lowest flow rate ($Re = 2600$) exhibits negative radial velocities at larger z/d , as would be expected for a contracting jet. The maximum negative radial velocity occurs approximately 0.4 diameters above the impingement plate. The velocity gradient distribution for the low Re data are illustrated in Fig. 4, where the open symbols indicate data normalized by the jet exit conditions, V_j and d . Since the low- Re jet accelerated and contracted before reaching the plate, V_j and d would not be expected to be appropriate for use in the dimensionless parameters (z/d , r/d , u/V_j , and Re). The

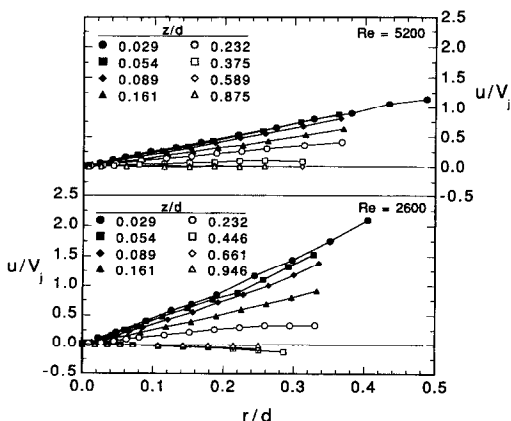


FIG. 3. Low Reynolds-number profiles of the mean radial velocity, $d = 14.0$ mm.

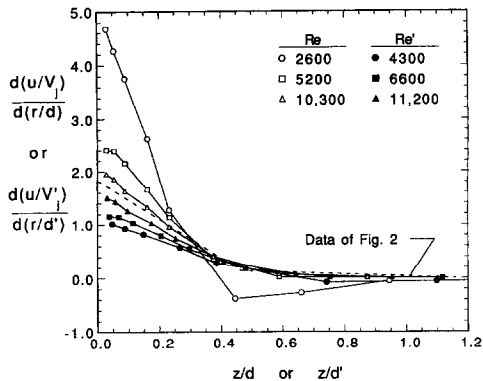


FIG. 4. Mean radial velocity gradient dependence on z/d for low Reynolds number jets.

dashed line represents a least-squares fit of the band of data of Fig. 2. As expected, the low Re data fall far outside the band of higher Re data if the effect of gravity is neglected. Since the nozzle-to-plate spacing was one diameter, an adjusted arrival velocity, V'_j , was determined from the Bernoulli equation for a distance of one nozzle diameter from the jet exit. A corresponding constricted jet diameter, d' , was calculated from continuity considerations. These data are also shown in Fig. 4 in dimensionless terms normalized by V'_j and d' ($Re' = V'_j d'/\nu$). The use of these contraction adjustments over-corrects the data. The assumption that the jet accelerates all the way to the plate introduces significant error in the dimensionless gradient calculation. Indeed, a normalization procedure which provides for the low Reynolds number data to lie in the same band as the high Re data suggests that the jet accelerates to within approximately half the jet diameter from the impingement plate [9]. This is consistent with the data of Fig. 2 and accompanying analysis.

CONCLUSIONS

Radial mean velocities in the stagnation region of pipe-type nozzles ($0 < z/d < 1.0$ and $0 < r/d < 0.5$) were found to vary linearly with the radial coordinate for a given axial location. The dimensionless velocity gradient, $d(u/V_j)/d(r/d)$, was found to be linear in z/d . A stream function was presented which describes the measured velocity field. An estimate was made for the point where jet deceleration begins due to the presence of the plate. Limited data from lower Reynolds number jet flows were considered and found to support the estimate of the point of initial jet deceleration.

Acknowledgements—This work was supported by the U.S. National Science Foundation under Grant No. CBT-8552493.

REFERENCES

1. H. Schlichting, *Boundary-Layer Theory*. McGraw-Hill, New York (1979).
2. F. M. White, *Viscous Fluid Flow*. McGraw-Hill, New York (1974).
3. R. G. Olsson and E. T. Turkdogan, Radial spread of a liquid stream on a horizontal plate, *Nature* **211**, 813–816 (1966).
4. T. Azuma and T. Hoshino, LDV measurement in radial flow of thin liquid film, *Proceedings of the Osaka Symposium on Flow Measuring Techniques: The Application of LDV*, Association for the Study of Flow Measurements, Osaka, Japan, pp. 1–15 (1983).
5. J. Stevens and B. W. Webb, Measurements of the free

- surface flow structure under an impinging, free liquid jet, *ASME J. Heat Transfer* **114**, 79–84 (1992).
6. J. Stevens and B. W. Webb, Measurements of flow structure in the radial layer of impinging free surface liquid jets, *Int. J. Heat Mass Transfer* **36**, 3751–3758 (1993).
 7. J. Stevens, Y. Pan and B. W. Webb, Effect of nozzle configuration on transport in the stagnation zone of axisymmetric impinging free liquid jets: Part 1. Turbulent flow structure, *ASME J. Heat Transfer* **114**, 874–879 (1992).
 8. Y. Pan, J. Stevens and B. W. Webb, Effect of nozzle configuration on transport in the stagnation zone of axisymmetric impinging free liquid jets: Part 2. Local heat transfer, *ASME J. Heat Transfer* **114**, 880–886 (1992).
 9. J. Stevens, Measurements of local fluid velocities in an axisymmetric, free liquid jet impinging on a flat plate, Ph.D. Dissertation, Brigham Young University, Provo, Utah (1991).
 10. J. Stevens and B. W. Webb, Local heat transfer coefficients under an axisymmetric, single-phase liquid jet, *ASME J. Heat Transfer* **113**, 71–77 (1991).
 11. X. Liu, L. A. Gabour and J. H. Lienhard V, Stagnation-point heat transfer during impingement of laminar liquid jets: analysis including surface tension, *ASME J. Heat Transfer* **115**, 99–105 (1993).